Photon–phonon-assisted tunneling through a double quantum dot molecule

2007 J. Phys.: Condens. Matter 19 496216

(http://iopscience.iop.org/0953-8984/19/49/496216)

IOP PUBLISHING JOURNAL OF PHYSICS: CONDENSED MATTER

J. Phys.: Condens. Matter **19** (2007) 496216 (10pp) doi:10.1088/0953-8984/19/49/496216

Photon–phonon-assisted tunneling through a double quantum dot molecule

Jing Wang, Xin Lu and Chang-Qin Wu[1]

Department of Physics, Fudan University, Shanghai 200433, People's Republic of China

E-mail: cqw@fudan.edu.cn

Received 7 June 2007, in final form 25 October 2007
Published 15 November 2007
Online at stacks.iop.org/JPhysCM/19/496216

Abstract

We investigate photon–phonon-assisted tunneling through a double quantum dot molecule using a well-established non-equilibrium Green function technique. The molecule is sandwiched between two ideal electrodes and the electron at each dot of the molecule interacts independently with Einstein phonons. The many-body problem of electron–phonon interactions is mapped onto a multichannel one-body problem. Together with these resonant peaks of the two-level system, additional satellite peaks due to the photon absorption (emission) process and/or phonon-assisted tunneling are observed in the transmission spectrum. Furthermore, the time-average current and differential conductance are calculated. The feasibility of manipulating the phonon-assisted tunneling with photon absorption (emission) processes by the voltage bias is also discussed.

1. Introduction

The advancement of nano-technology in the last decade has made it possible to design nano-scale single-molecular devices based on quantum dot (QD) structures with controllable size and shape. Experiments based on these single-molecular systems open up a new view of quantum signal processing as well as quantum optical and electrical processes, and as a result of the definite evidence of quantum transport in these systems the properties of tunneling through a mesoscopic system have regained dramatic theoretical [1–12] and experimental [13–15] interest. Theoretical efforts have been made to describe the physical mechanisms of the tunneling, and a variety of methods, including the Green function techniques [3–6], the Fermi golden rule [7–9], and non-equilibrium linked cluster expansion [10], have been well developed to address the related concerns. Electron–phonon interaction (EPI) is of the great importance in the tunneling event within the quantum dot molecule [15–18].

A double coupled QD system sandwiched between two ideal leads with dot–dot and dot–lead coupling could be taken as a good artificial molecule model for studying the mescoscopic

[1] Author to whom any correspondence should be addressed.

tunneling properties, as the energy level in such a multiple gated structure could be designed for the strength of the interdot coupling and the tunneling rate for the leads [14–18] while the electron occupation of the states could be manipulated by the dc bias voltage [15, 16]. The many-body problem in a system with some inelastic scattering process, such as phonon absorption/emission, could be mapped onto a solvable multichannel single-electron scattering problem as done first by Bonca and Trugman [2]. With this technique, some theoretical investigations of phonon effects on the electron tunneling through mesoscopic systems with electron–phonon interaction have been reported [2, 3, 8, 11, 12], where the electron–phonon interaction is described either by the Holstein model [19] (where the electrons are coupled with an Einstein phonon mode at each site) or by the Su–Schreiffer–Heeger (SSH) model [20] (where the electrons are coupled with the phonon modes on bonds). In a previous work [1], the present authors discussed the tunneling properties in the double QD system with electron–phonon interaction and found the peaks of the differential conductance according to the phonon-assisted tunneling.

In the presence of a microwave (MW) irradiation field, photon absorption/emission processes were reported to be influential on the tunneling in a single QD molecule, and a theoretical work [7] found that together with the EPI, the photon absorption/emission would induce additional peaks in the nonlinear differential conductance. Recent quantum transport measurements on a double QD molecule with external microwave irradiation demonstrated the existence of a photon-assisted tunnel (PAT) [16], providing us a new viewpoint for understanding the essence of the influence of EPI on the transport properties in the molecule. Theoretically, the tunneling through the double QD system with EPI in the presence of a MW field could be treated with the same method used by Dong *et al* [7] in a single QD system. With this method, the many-body problem could be transformed exactly into a one-body scattering problem with representation of the original Hamiltonian in the electron–phonon coupled Fock space [2]. Further, the time-dependent and time-average transmissivity and current could be calculated by the non-equilibrium Green function in the framework of Büttiker scattering theory.

In this work we focus on the photon–phonon-assisted tunneling effect in a coupled double QD molecule. We use the nonlinear Green function to calculate the differential conductance and time average current with extension of the method to a single QD molecule and discuss the contribution of the photon absorption/emission processes on the tunneling effect in a double QD molecule. In this study, the inelastic processes due to phonon absorption/emission are addressed by the Holstein model and the irradiation microwave field is treated with the adiabatic approximation. Compared with our previous study on phonon-assisted tunneling in a similar model without an external microwave irradiation field [1], we focus on the effect of photon absorption/emission on tunneling through a double coupled QD system as well as its effects on the phonon-assisted resonances.

The rest of the paper is organized as follows. In section 2 we introduce the Hamiltonian for resonant tunneling and review the main result of the Keldysh theory, used in this work. In section 3 we give the numerical results from the calculation within the framework given in section 2. In section 4 we give a summary of our results with a brief discussion.

2. Theoretical method

The Hamiltonian H of the system we considered in this work can be written as follows [1, 7]:

$$H = H_M + H_{\text{lead}} + H_{\text{int}}, \tag{1a}$$

where

$$H_M = \omega_0 \sum_{i=1}^{2} b_i^\dagger b_i - t(c_1^\dagger c_2 + c_2^\dagger c_1) + \lambda \sum_{i=1}^{2} c_i^\dagger c_i (b_i^\dagger + b_i), \tag{1b}$$

describes a double QD molecule, in which each dot has a single electronic level and the electron at the level couples with an Einstein phonon mode (with the same phonon frequency ω_0), ${c_i}^\dagger$ (c_i) denotes the electron creation (annihilation) operator on site i and $b_i^\dagger$ (b_i) for the phonon modes ($i = 1, 2$), t is the hopping constant between the two dots and λ is the coupling between the electron and phonon at the same site. The second term of the Hamiltonian H

$$H_{\text{lead}} = \sum_{k,\eta\in L,R} \epsilon_{k\eta}(t) c_{k\eta}^\dagger c_{k\eta}, \tag{1c}$$

describes the two isolated leads, $c_{k\eta}^\dagger$ ($c_{k\eta}$) creates (annihilates) an electron with momentum k in the $\eta(= L/R)$ lead. The MW field irradiating the leads is described by a rigid shift of the single-electron energy spectrum under the adiabatic approximation $\epsilon_{k\eta}^0 \to \epsilon_{k\eta}(t) = \epsilon_{k\eta}^0 + \Delta_\eta(t)$ ($\Delta_\eta(t) = \Delta_\eta \cos \Omega t$), where $\epsilon_{k\eta}^0$ is the time-independent single electron energy without a MW field. Δ_η is the irradiation strength and Ω is the frequency of the MW field. The last term in the Hamiltonian H is the interaction between the molecule and the leads

$$H_{\text{int}} = V_{kL,1}(c_{kL}^\dagger c_1 + \text{H.c.}) + V_{kR,2}(c_{kR}^\dagger c_2 + \text{H.c.}), \tag{1d}$$

where $V_{k\eta,i}$ stands for the tunneling coupling between the molecule and the ηth lead.

The transport property can be meaningfully defined as a multichannel scattering problem [2], for which we define a polaron state [2, 7, 8, 11]

$$|i, n_1, n_2\rangle = c_i^\dagger \frac{(b_1^\dagger)^{n_1}}{\sqrt{n_1!}} \frac{(b_2^\dagger)^{n_2}}{\sqrt{n_2!}} |0, 0\rangle, \qquad (n_1, n_2 \geqslant 0, i = 1, 2), \tag{2}$$

where the electron occupies the ith dot and there are n_1 and n_2 phonons in the two dots in the molecule, respectively. Similarly,

$$|k\eta, n_1, n_2\rangle = c_{k\eta}^\dagger \frac{(b_1^\dagger)^{n_1}}{\sqrt{n_1!}} \frac{(b_2^\dagger)^{n_2}}{\sqrt{n_2!}} |0, 0\rangle, \qquad (n_1, n_2 \geqslant 0, i = 1, 2) \tag{3}$$

describes the many-body system of the leads consisting of a single electron with n_1 and n_2 phonon excitations on two dots, respectively. It should be noted that such definitions in equations (2) and (3) map a many-body problem onto a multichannel one-body problem, where only one particle exists in the whole system. The pseudo-channel α weighted by the probability $P(\alpha) = P(n_1)P(n_2)$ with $P(n_i) = (1 - \mathrm{e}^{-\beta\omega_0})\mathrm{e}^{-n_i\beta\omega_0}$ ($i = 1, 2$), which is a probability of the phonon number state $|n_1, n_2\rangle$ at finite temperature T. Furthermore we write these Dirac brackets as operators [7, 8]:

$$c_{i,n_1,n_2}^\dagger = |i, n_1, n_2\rangle, \qquad c_{k\eta,n_1,n_2}^\dagger = |k\eta, n_1, n_2\rangle.$$

Then we could map the many-body problem onto a single-particle problem [2, 3, 7, 8, 11], and obtain the effective Hamiltonian as

$$\begin{aligned} H_{\text{eff}} = \sum_{n_1,n_2} \{ & \omega_0 (n_1 c_{1,n_1,n_2}^\dagger c_{1,n_1,n_2} + n_2 c_{2,n_1,n_2}^\dagger c_{2,n_1,n_2}) - t(c_{1,n_1,n_2}^\dagger c_{2,n_1,n_2} + \text{H.c.}) \\ & + \lambda\sqrt{n_1+1}(c_{1,n_1+1,n_2}^\dagger c_{1,n_1,n_2} + \text{H.c.}) + \lambda\sqrt{n_2+1}(c_{2,n_1,n_2+1}^\dagger c_{2,n_1,n_2} + \text{H.c.})\} \\ & + \sum_{k\eta,n_1,n_2} \epsilon_{k\eta,n_1,n_2}(t) c_{k\eta,n_1,n_2}^\dagger c_{k\eta,n_1,n_2} \\ & + \sum_{k,n_1,n_2} \{V_{kL,1}^{n_1,n_2}(c_{kL,n_1,n_2}^\dagger c_{1,n_1,n_2} + \text{H.c.}) + V_{kR,2}^{n_1,n_2}(c_{kR,n_1,n_2}^\dagger c_{2,n_1,n_2} + \text{H.c.})\}, \end{aligned} \tag{4}$$

with $\epsilon_{k\eta,n_1,n_2}(t) = \epsilon_{k\eta,\alpha}(t) = \epsilon_{k\eta}(t) + \alpha\hbar\omega_0$. $V^{n_1,n_2}_{k\eta,i}(= V^{\alpha}_{k\eta,i})$ is the coupling between the αth ($|n_1, n_2\rangle$) pseudo-channel in the η lead and the coupled QDs. Naturally, the Hamiltonian is infinite; we can truncate the Fock space by allowing a certain number of phonons for each mode to obtain a very accurate solution. The explicit commutators of these operators can be easily established from the definition of these Dirac brackets [7]:

$$\{c_{i,n_1,n_2}, c^{\dagger}_{j,m_1,m_2}\} = \delta_{ij}\delta_{n_1m_1}\delta_{n_2m_2}, \qquad \{c_{k\eta,n_1,n_2}, c^{\dagger}_{k\eta',m_1,m_2}\} = \delta_{\eta\eta'}\delta_{n_1m_1}\delta_{n_2m_2}.$$

Starting from the effective Hamiltonian of equation (4), the transport property through the mesoscopic structure can be described by the non-equilibrium Keldysh Green function [21–23] and the tunneling current $J_{L\alpha}(t)$ is given as:

$$\begin{aligned} J_{L\alpha}(t) &= \frac{ie}{\hbar}\sum_k [V^{\alpha}_{kL,1}\langle c^{\dagger}_{kL,\alpha}c_{1,\alpha}\rangle - V^{\alpha *}_{kL,1}\langle c^{\dagger}_{1,\alpha}c_{kL,\alpha}\rangle] \\ &= \frac{ie}{\hbar}\sum_k [V^{\alpha}_{kL,1}G^{(\alpha,\alpha)<}_{1,kL}(t,t) - V^{\alpha *}_{kL,1}G^{(\alpha,\alpha)<}_{kL,1}(t,t)]. \end{aligned}$$

Using the Keldysh Green function, one has the Dyson equation

$$G^{(\alpha,\alpha)<}_{i,kL}(t,t') = \sum_{j=1}^{2}\int dt_1\, V^{\alpha *}_{kL,j}[G^{(\alpha,\alpha)r}_{ij}(t,t_1)g^{(\alpha,\alpha)<}_{kL}(t_1,t') + G^{(\alpha,\alpha)<}_{ij}(t,t_1)g^{(\alpha,\alpha)a}_{kL}(t_1,t')],$$

in which $g^{(\alpha,\alpha)<,a}_{kL}$ are the free-electron Green functions in the αth pseudo-channel of lead L without coupling to the central region. In the steady state the Green function depends only on the time difference[2], so the Fourier transformation gives $G^{(\alpha,\alpha')r(a)}_{i,j}(\epsilon) = \langle\langle c_{i,\alpha}; c^{\dagger}_{j,\alpha'}\rangle\rangle^{r(a)}_{\epsilon}$ and $G^{(\alpha,\alpha')<(>)}_{i,j}(\epsilon) = \langle\langle c_{i,\alpha}; c^{\dagger}_{j,\alpha'}\rangle\rangle^{<(>)}_{\epsilon}$ [21].

By using the equation of motion (EOM) technique [25], we have

$$\begin{aligned} [\epsilon - n_1\hbar\omega_0 - n_2\hbar\omega_0 - \bar{\Sigma}^r_{n_1n_2}(\epsilon)]\bar{G}^{(n_1n_2,m_1m_2)r}_{1,j} &= \delta_{1,j}\delta_{n_1,m_1}\delta_{n_2,m_2} - t\bar{G}^{(n_1n_2,m_1m_2)r}_{2,j} \\ &\quad - \lambda\sqrt{n_1}\bar{G}^{(n_1-1n_2,m_1m_2)r}_{1,j} - \lambda\sqrt{n_1+1}\bar{G}^{(n_1+1n_2,m_1m_2)r}_{1,j}, \end{aligned} \tag{5}$$

$$\begin{aligned} [\epsilon - n_1\hbar\omega_0 - n_2\hbar\omega_0 - \bar{\Sigma}^r_{n_1n_2}(\epsilon)]\bar{G}^{(n_1n_2,m_1m_2)r}_{2,j} &= \delta_{2,j}\delta_{n_1,m_1}\delta_{n_2,m_2} - t\bar{G}^{(n_1n_2,m_1m_2)r}_{1,j} \\ &\quad - \lambda\sqrt{n_2}\bar{G}^{(n_1n_2-1,m_1m_2)r}_{2,j} - \lambda\sqrt{n_2+1}\bar{G}^{(n_1n_2+1,m_1m_2)r}_{2,j}. \end{aligned} \tag{6}$$

In the absence of a MW field, the retarded self-energies in the above equations due to the tunneling into the electric leads are given by

$$\bar{\Sigma}^r_{\alpha}(\epsilon) = \sum_{k\eta,n}\frac{|V^{\alpha}_{k\eta,i}|^2}{\epsilon - \epsilon^0_{k\eta} - \alpha\hbar\omega_0 + i0^+}. \tag{7}$$

Here we have neglected the level shift and assumed the line widths to be energy-independent constants, $\bar{\Sigma}^r_{\alpha}(\epsilon) = -\frac{i}{2}(\Gamma_L + \Gamma_R) = -\frac{i}{2}\Gamma$. The approximation we take to truncate the EOM is identical to the one used by Meir, Wingreen, and Lee [26] for the Anderson impurity model without an ac field [7, 27].

In the presence of a MW field, the Keldysh Green function has the form

$$G^{(\alpha,\alpha)<(>)}(t,t') = \sum_{\eta,\alpha'}\int\frac{d\epsilon}{2\pi}e^{-i\epsilon(t-t')-i\int_{t'}^{t}d\tau\Delta_{\eta}(\tau)}\Sigma^{<(>)}_{\eta,\alpha}(\epsilon)A^{(\alpha,\alpha')r}_{\eta}(\epsilon,t)[A^{(\alpha,\alpha')r}_{\eta}(\epsilon,t')]^*, \tag{8}$$

[2] In the general non-equilibrium situation, all the Green functions depend separately on the two tie variables t and t'. However, since we are interested here in a stationary situation they depend only on $(t - t')$.

where

$$A_{\eta}^{(\alpha,\alpha')r}(\epsilon,t) = \int_{-\infty}^{t} \mathrm{d}t_1 \int \frac{\mathrm{d}\epsilon'}{2\pi} \mathrm{e}^{\mathrm{i}(\epsilon'-\epsilon)(t-t_1)-\mathrm{i}\int_{t_1}^{t} \mathrm{d}\tau\,\Delta_\eta(\tau)} \bar{G}^{(\alpha,\alpha')r}(\epsilon')$$
$$= \exp\left[-\mathrm{i}\frac{\Delta_\eta}{\Omega}\sin\Omega t\right] \sum_{l=-\infty}^{\infty} J_l\left(\frac{\Delta_\eta}{\Omega}\right) \bar{G}^{(\alpha,\alpha')r}(\epsilon - l\Omega). \tag{9}$$

Here J_l is the lth order Bessel function. After some algebra, we obtain

$$J(t) = \frac{e}{h}\Gamma_{\mathrm{L}}\Gamma_{\mathrm{R}} \int \mathrm{d}\epsilon\, \Sigma_{\alpha,\alpha'} |A_{\mathrm{R}}^{(\alpha,\alpha')r}|^2 \{P_\alpha f_{\mathrm{L}}^{\alpha}(\epsilon)[1 - f_{\mathrm{R}}^{\alpha'}(\epsilon)] - P_{\alpha'} f_{\mathrm{R}}^{\alpha'}(\epsilon)[(1 - f_{\mathrm{L}}^{\alpha})]\}, \tag{10}$$

where $f_{\eta}^{\alpha}(\epsilon) \equiv [1 + \exp(\epsilon + \alpha\hbar\omega_0 - \mu_\eta)/k_{\mathrm{B}}T]^{-1}$ is the Fermi distribution function of the αth pseudo-channel in the η lead, μ_η is the chemical potential that is different for the left and right leads upon a voltage bias V, i.e. $\mu_{\mathrm{L}} - \mu_{\mathrm{R}} = eV$. This gives the average incident current at a probe in terms of total reflection and transmission probabilities. Meanwhile, we have the transmission rate in the presence of the MW field:

$$T_{\mathrm{tot}}(\epsilon) = \Gamma_{\mathrm{L}}\Gamma_{\mathrm{R}} \sum_{\alpha,\alpha'} P_\alpha \sum_{l=-\infty}^{\infty} J_l^2\left(\frac{\Delta_{\mathrm{R}}}{\Omega}\right) |\bar{G}_{\mathrm{L}\to\mathrm{R}}^{(\alpha,\alpha')r}(\epsilon)|^2. \tag{11}$$

3. Numerical results

Numerical results have been obtained for the coupled double QD molecule both in the absence and in the presence of a MW irradiation field. For simplicity, we consider that the tunneled coupling between the double QD molecule and the two leads is symmetric $\Gamma_{\mathrm{L}} = \Gamma_{\mathrm{R}} = \Gamma/2$, with the same MW field intensity $\Delta_{\mathrm{L}} = \Delta_{\mathrm{R}} = \Delta$ [24]. In our calculation the interdot hopping $t = 1$ is set as the unit of energy. The maximum number of allowed phonon quanta N_{phonon} is chosen in relation to the energy of the Einstein phonon mode, the EPI constant, and the temperature of the system under investigation. As we are concerned with these parameters in the present paper, we choose $N_{\mathrm{phonon}} = 5$, which gives convergent results.

3.1. Transmission probability

In figure 1 we show the total transmission rate as a function of the incoming electron energy ϵ at zero temperature under different MW irradiation fields with a fixed intensity $\Delta = 0.8$. The pairs of numbers $(N_{\mathrm{photon}}, N_{\mathrm{phonon}})$ located around the peaks indicate the number of photons that the electron absorbs (positive) or emits (negative) and the mean number of excited phonons ($\langle b^\dagger b\rangle$) [1], respectively. In the absence of phonons and photons there are two resonant peaks at $\epsilon = \pm 1$ in the energy spectrum which represent the bonding and anti-bonding resonant energy levels. We first consider the case in which there exists only the time-dependent potential $\epsilon(t)$ which drives the central molecule. The result is shown as a solid line in figure 1(a). We see that the two main resonant peaks are unaffected by the MW field, while some side peaks appear symmetrically around the two peaks at the position $\epsilon' = \epsilon \pm N_{\mathrm{photon}}\Omega$, ($N_{\mathrm{photon}} = 0, \pm 1, \pm 2, \ldots$) since the electron could absorb or emit photons during the process. The heights of the satellite peaks decrease while more photons are emitted or absorbed. Pure photon absorption peaks can be seen in the left side of the resonant regime due to the fact that photon mode is independent of temperature, in contrast with the phonon case [1].

For a comparison, we now see the case without a MW field but with e–p interaction; we show the result as a dashed line in figure 1(a). The energy shift of the resonant peaks is due

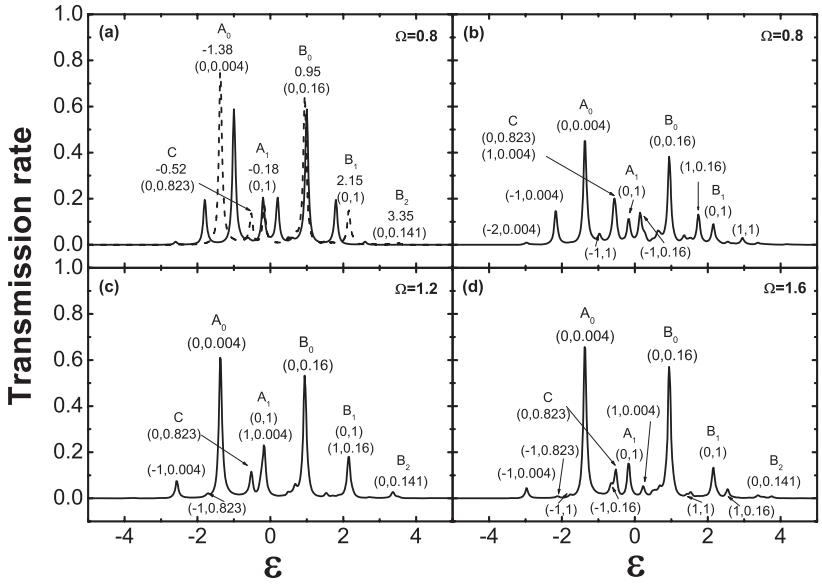

Figure 1. Transmission rate as a function of incident electron energy for different irradiations at zero temperature. As a comparison, in (a) we show the result when the e–p interaction is turned off (solid line) and when no MW field is present (dashed line). The intensity of the irradiation is fixed at $\Delta = 0.8$. The pair of numbers in brackets denotes the numbers for emission (positive) or absorption (negative) of photons and phonons, respectively, involved in the tunneling process. The numbers above these brackets in (a) give the value of incident energies corresponding to these peaks. The model parameters are taken as $\lambda = 0.8$, $\omega_0 = 1.2$ and $\Gamma = 0.05$.

to the polaron effect which is produced by the phonon cloud [1]. The magnitude of the shift increases with the increase of λ^2, as well as with the decrease of ω_0. At zero temperature there is no emission phonon mode on the energy spectrum. The peaks are located on the right side of the resonant peak because no phonon exists at the molecule before the scattering [4, 6, 10, 11]. The first resonant peak A_0 as well as other peaks in the series of A_n stay almost unchanged with different values of phonon frequency ω_0. But the resonant peak B_0 as well as other peaks in the series B_n are changed significantly. Our former work [1] has clearly interpreted such phenomena. Due to the symmetry of the two-dot exchange, the eigenstates are either symmetric or anti-symmetric. There is only level crossing between different symmetric states and no crossing for the states of the same symmetry. The two most weighted peaks in the transmission spectrum are not simply evolved from the two peaks in the absence of the e–p interaction. The first one (indicated by A_0) is caused by the first symmetric state, which is evolved from a bonding state. The energy of the resonant peak A_n is $\epsilon(A_n) = \epsilon_0 - t - \lambda^2/\omega_0 + n\omega_0$ which correspond to the first symmetric state with n phonons. Similarly the series of B_n with the energy $\epsilon(B_n) = \epsilon_0 + t - \lambda^2/\omega_0 + n\omega_0$ represents the processes accompanying the emission of n bare phonons. The peak C emerging at $\epsilon = -0.52$ is due to the first anti-symmetric state of the number of excited phonons, 0.823. The strength of the resonant transmission decreases with the increase in the number of excited phonons.

Now we turn to the case in which e–p interaction and the MW field are both turned on; a direct consequence is that many more resonant peaks are observed. Due to the process of one-photon emission from the state A_1, one new peak $(-1, 1)$ appears between the resonant peak A_0 and the first phonon satellite peak C for the case of lower MW frequency ($\Omega = 0.8 < \omega_0$ (figure 1(b))), which shows a qualitative agreement with the experiment result [16]. Since

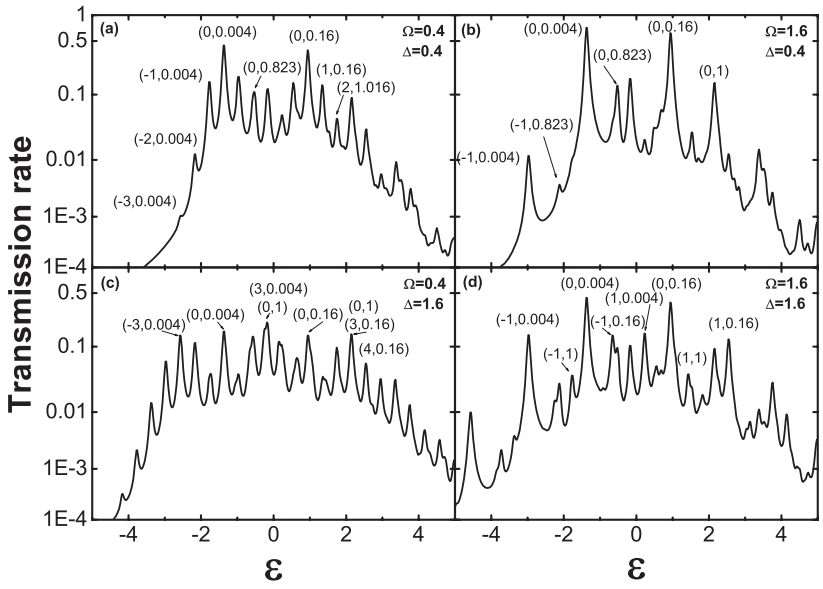

Figure 2. Transmission rate as a function of the incident electron energy calculated for different irradiations at zero temperature: in (a) and (c) the frequency of irradiation is $\Omega = 0.4$, lower than that of phonons; in (b) and (d) the frequency of irradiation is $\Omega = 1.6$, larger than that of phonons. The intensities of the irradiations are $\Delta = 0.4$ ((a), (b)) and $\Delta = 1.6$ ((c), (d)), respectively. All other parameters are the same as in figure 1. Please note that the transmission rate is shown on a logarithmic scale.

the first phonon satellite peak C is superposed by the first absorption state of the resonant peak A_0, the peak becomes more intense. The other phonon peaks are also accompanied by emission/absorption of photons. Such photon-assisted multi-phonon processes lead to the appearance of some new pseudo-channels that contribute to tunneling, as shown in figures 1(b)–(d). When the photon frequency Ω is equal to that of phonon frequency ω_0 in figure 1(c), the resonant peaks are superposed by both photon and/or phonon absorption/emission together. The one-phonon absorption peaks (A_1, B_1) in particular are greatly strengthened by the superposition of the corresponding one-photon absorption processes. If the frequency of the MW field is higher than that of the phonon, no phonon absorption process takes place between the main resonant phonon peak (A_0) and the first phonon peak (C) (see figure 1(d)) because there is insufficient energy exciting the higher frequency photon.

By comparing the time-average transmissions of two different intensities of the MW field, shown in figure 2, we can see more a complicated peak distribution appearing in the transmission spectrum. It is clearly seen that increasing the intensity of the MW field will enhance the photon-assisted processes. For example, for the MW fields of frequencies $\Omega = 0.4$ and 1.6 with intensity $\Delta = 0.4$ and 1.6, in figure 2, we obviously observe more peaks with higher amplitudes involving the emission and absorption of photons.

3.2. Current and differential conductance

We now calculate the current of the tunneling process for the system. In the first row of figure 3, we plot the time-average current as a function of the bias voltage V between the two leads. The Fermi level at the right lead was set to locate at $E_R = -5$ eV, and a bias voltage V was applied on the left lead (i.e. $\mu_L = E_R + eV$, $\mu_R = E_R$). The appearance of the steps in figure 3 indicates

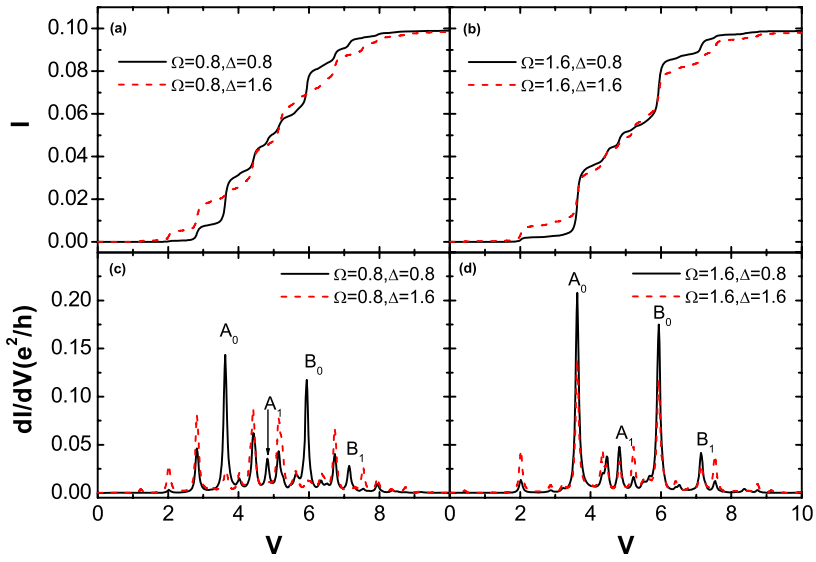

Figure 3. The time-average current I and the corresponding differential conductance $\mathrm{d}I/\mathrm{d}V$ as a function of the applied bias voltage under various irradiations. All other parameters are the same as in figure 1.

(This figure is in colour only in the electronic version)

the existence of new satellite peaks in transmission due to the tunneling process discussed above. As mentioned above, more photon–phonon-assisted tunneling resonances are observed when the intensity of ac field is stronger, which is clearly seen in the first row of figure 3.

In the second row of figure 3, we show the differential conductance $(\mathrm{d}I/\mathrm{d}V)$ with the same model parameters and external field as the corresponding figures in the first row. Due to its proportionality to $T_{\mathrm{tot}}(eV)$, the differential conductance $(\mathrm{d}I/\mathrm{d}V)$ plotted as functions of the voltage in figure 3 exhibits resonant peaks corresponding to the peaks at $\epsilon = eV + E_{\mathrm{R}}$ in figure 2. As one can see, the differential conductance is more distinguishable for the resonant transmission (shown as peaks) than in the I–V curve (shown as steps). That implies that a possible way to experimentally demonstrate the photon–phonon-assisted tunneling may be by measuring the differential conductance $\mathrm{d}I/\mathrm{d}V$. Integrating the total transmission probability over incident energies, $\int \mathrm{d}\epsilon\, T_{\mathrm{tot}}(\epsilon)$ is independent of electron–phonon interaction and the presence of a MW irradiation field, which indicates that a sum rule exists in the differential conductance. Here we assume that the voltage bias is sufficiently high and all the filled states in the two leads are taken into account. The height of the resonant peaks is greatly manipulated by the intensity of the MW field. In figure 3(c), one clearly sees that the two main resonant peaks (A_0, B_0) and the two corresponding one-phonon peaks (A_1, B_1) are obviously weakened, while those of photons are greatly strengthened for the large-intensity case. That is not so obvious for a large photon energy ($\Omega = 1.6$) in figure 3(d) due to the sum rule. Increasing the intensity of the MW field, the resonant peaks due to the photon absorption or emission are enhanced while all other peaks irrelevant to photons are depressed concurrently.

The microwave spectroscopy experiments on the double QD devices could be applied to test the results in our work. The current and differential conductance as functions of bias voltage in an artificial molecule of double coupled QD system under microwave irradiation could be taken in comparison with the curves in this study. Though the same experiment

is not available now, some previous experimental work on the transport properties of double QD devices could be taken, such as [16–18], and our results show good qualitative agreement with the literature. Fujisawa *et al* observed phonon-assisted satellite peaks in the differential conductance spectrum ($-\mathrm{d}I/\mathrm{d}\varepsilon$ figure 3(A) in [18]) which could be explained by the results of phonon-assisted tunneling in our work; in the study of MW spectroscopy of double QD devices from the same group [17], the MW photon frequency-dependent double peaks appear on the current curves as a function of the voltage of the left QD (figure 1(c) in [17]), which is similar to our calculation results (figure 1(a)); Qin *et al* observed the superposition of the photon- and phonon-assisted tunneling phenomena very recently [16]. Moreover, in order to observe the photon–phonon-assisted tunneling phenomena unambiguously, the experiment should be performed at an extremely low temperature as the thermal effect may cause a decrease of the differential conductance and a low signal/noise ratio.

4. Summary

In summary, we have discussed the low-temperature time-dependent resonant tunneling through a double QD system coupled to a local phonon mode in a MW field theoretically. The method of the photon–phonon-assisted tunneling in a single QD system proposed by Dong *et al* [7] was expanded to a coupled double QD system by projecting the original Hamiltonian in the representation of electron–phonon coupled Fock space. The time-average current and differential conductance calculated by the NGF method exhibits peaks of the phonon-assisted and photon–phonon-assisted tunneling through the double QD system with MW field radiation. The processes of phonon emission and absorption are of great importance to the tunneling in the quantum system with an external MW field that is also controllable by an adjustable bias voltage.

Acknowledgments

This work was supported by the National Natural Science Foundation of China, the Ministry of Science and Technology of China (through grant no. 2006CB921302), and the EC Project OFSPIN (NMP3-CT-2006-033370).

References

[1] Lu X, Wang J and Wu C Q 2006 *Eur. Phys. J.* B **49** 325
[2] Bonča J and Trugman S A 1995 *Phys. Rev. Lett.* **75** 2566
[3] Vasilevskiy M I, Anda E V and Makler S S 2004 *Phys. Rev.* B. **70** 035318
[4] Wingreen N S, Jacobsen K W and Wilkins J W 1989 *Phys. Rev.* B **40** 11834
[5] Jauho A P, Wingreen N S and Meir Y 1994 *Phys. Rev.* B **50** 5528
[6] Zhu J X and Balatsky A V 2003 *Phys. Rev.* B **67** 165326
[7] Dong B, Cui H L and Lei X L 2004 *Phys. Rev.* B **69** 205315
[8] Dong B, Cui H L, Lei X L and Horing N J M 2005 *Phys. Rev.* B **71** 045331
[9] Mourokh L G, Horing N J M and Smirnov A Y 2002 *Phys. Rev.* B **66** 085332
[10] Král P 1997 *Phys. Rev.* B **56** 7293
[11] Haule K and Bonča J 1999 *Phys. Rev.* B. **59** 13087
Bonča J and Trugman S A 1997 *Phys. Rev. Lett.* **79** 4874
[12] Emberly E G and Kirczenow G 2000 *Phys. Rev.* B **61** 5740
[13] Stoof T H and Nazarov Y V 1996 *Phys. Rev.* B **53** 1050
[14] Van der Wiel W G, De Franceschi S, Elzerman J M, Fujisawa T, Tarucha S and Kouwenhoven L P 2003 *Rev. Mod. Phys.* **75** 1
[15] Fujisawa T, Van der Wiel W G and Kouwenhoven L P 2000 *Physica* E **7** 413

[16] Qin H, Holleitner A W, Eberl K and Blick R H 2001 *Phys. Rev.* B **64** 241302
[17] Oosterkamp T H, Fujisawa T, van der Wiel W G, Lshibashi K, Hijman R V, Tarucha S and Kouwenhoven L P 1998 *Nature* **395** 873
[18] Fujisawa T, Oosterkamp T H, van der Wiel W G, Broer B W, Aguado R, Tarucha S and Kouwenhoven L P 1998 *Science* **282** 932
[19] Holstein T 1959 *Ann. Phys.* **8** 325
Holstein T 1959 *Ann. Phys.* **8** 343
[20] Su W P, Schrieffer J R and Heeger A J 1979 *Phys. Rev. Lett.* **42** 1698
[21] Caroli C, Combescot R, Nozieres P and Saint-James D 1971 *J. Phys. C: Solid State Phys.* **4** 916
Caroli C, Combescot R, Nozieres P and Saint-James D 1972 *J. Phys. C: Solid State Phys.* **5** 21
[22] Manhan G D 1981 *Many Particle Physics* (New York: Plenum)
[23] Meir Y and Wingreen N S 1992 *Phys. Rev. Lett.* **68** 2512
[24] Büttiker M, Prêtre A and Thomas H 1993 *Phys. Rev. Lett.* **70** 414
[25] Schwinger J 1970 *Quantum Kinematics and Dynamics* (New York: Benjamin)
[26] Meir Y, Wingreen N S and Lee P A 1991 *Phys. Rev. Lett.* **66** 3048
[27] Ng T K 1996 *Phys. Rev. Lett.* **76** 487